

## Beyond of the Experimental Limit of SIMS In-Depth Resolution

M. Boulakroune and D. Benatia

Department of Electronic's, Faculty of Engineer Sciences,  
University Colonel Hadj Lakhdar of Batna, Batna-05000, Algeria

**Abstract:** In this study, we describe the improvement of the in-depth resolution of SIMS analysis. So, an algorithm post-erosion is used in order to deconvolve some simulated and real SIMS profiles. The simulated profiles are chosen so that they correspond to real cases encountered by the SIMS analyst and clarify what can be expected from the method. The real SIMS profiles are obtained by analysis of delta-layers of boron-doped silicon in a silicon matrix, analyzed in a Cameca Ims6f at oblique angle incidence. It is shown that the in-depth resolution is improved by a mean factor, in almost of cases, supper than 3 and the shape of both profiles experimental and simulated is retrieved in a very satisfactory way.

**Key words:** SIMS, in-depth resolution, DRF, deconvolution, silicon matrix, wiener algorithm

### INTRODUCTION

SIMS, secondary ion mass spectrometry, is the most sensitive of the techniques for surface analysis. One of its most important applications is the characterization of materials with detection limits at the part per million and part per billion levels (Kawashima *et al.*, 2004; Boulakroune and Berrabah, 2001). Its provision of compositions-depth profiles has had an enormous impact on the evaluation of thin films and surfaces coatings. Concentration-depth profiling by SIMS of dopant in semiconductors has become essential in the evaluation of the various stages in semiconductor processing. The technique is now used widely for quality control. However, the SIMS technique is a destructive one, also the material is never removed layer by layer as would be required for an ideal analysis. A number of factors can be responsible for the degradation of the depth profiles, including ion-induced surface topography, collisional mixing, preferential sputtering, ion implantation, segregation and diffusion (Aitkaki *et al.*, 2002). Also, after ion bombardment of smooth surfaces, other surface features can appear which contributes to an uncertainty as to the precise location of the reference surface and hence also to the depth profiles (Shao *et al.*, 2004). Thus, care is needed in interpreting the results from sputter profiling which can be both material and beam dependent.

The depth resolution obtained in SIMS depth profiles is similar in concept to that obtained in depth using the other surface analysis techniques relying upon sputtering to remove successive surface layers. The depth resolution

of SIMS profiles is degraded by poor instrumental alignment and sample roughness (Hofmann, 2001; Wu, 2006). However, even if perfectly flat samples are analyzed with an ideally aligned system, some deviations from the true profile can occur. The precise mechanisms of the profile-broadening effects observed are, generally, result from the collision cascade induced in the sample surface by the bombarding primary ions. As long as the bombardment does not produce any micro-topography roughness, the depth resolution should remain a function of the primary ion energy only (Yang and Goodman, 2006).

In a magnetic sector instrument at low primary beam energy, the SIMS depth resolution in silicon samples is governed mostly by the collisional mixing and in the case of an oxygen primary beam by the incorporation of the primary oxygen ions in the matrix of the sample (swelling) (Gautier *et al.*, 1996). Those phenomena which are responsible for the artificial broadening of the profiles, are inherent in the measurement process and can only be limited by improving the performances of a SIMS instrument. Owing to well-known SIMS limitations the measured profiles are broader than the actual profiles, especially at the decaying part. Furthermore, the SIMS profiles exhibit an energy-depend shift (Herzel *et al.*, 1995; Shao *et al.*, 2004; Hofmann, 2001; Wu, 2006). These limitations can be reduced by lowering the primary energy, but this increases the measurement time. Moreover, the development of more and more sophisticated instrumentation might give rise to an increase in the skills of SIMS operators, which is already very high

(Gautier *et al.*, 1996). Fortunately, the deformation of the profile by the measurement, as well as its shift, can be partly undone by a mathematical procedure called deconvolution. Deconvolution will not replace either a good experiment nor instrumental improvements which are obviously the only way toward the best resolution, but it allows better depth resolution to be reached from a careful analysis. A deconvolution procedure can therefore be used in order to retrieve the original signal, blurred by a linear and invariant Depth Resolution Function (DRF). The aim of this study is to present results on the improvement of SIMS in-depth resolution. The first step of this work is the determination of the response system DRF in the case of boron-doped silicon in a silicon matrix, analyzed in a Cameca Ims6f at oblique angle incidence and fitted this function with an analytical expression initially proposed by Dowsett *et al.* (1994). Then, we have used this analytical depth resolution for the implementation of SIMS profiles simulation, we have performed the deconvolution of simulated profiles in order to test the possibilities of the algorithm. Finally the deconvolution of boron multilayer profiles is presented.

### IN-DEPTH RESOLUTION

**Definition and measurement:** The in-depth resolution characterizes the precision of a profile. Roughly speaking, it is the range in units of sputtered depth which limits the knowledge of a variation in composition of a sample. This corresponds to the measured interface width when sputtering through an atomically sharp A/B interface. The generally accepted definition of the depth resolution  $\Delta z$  is the sputtered depth resolution between 84 and 16% of the plateau intensity of the analyzed component. This  $\Delta z$  (84-16%) has been used by the majority of authors and is recommended by IUPAC and the ASTM- E42 committee (Gautier *et al.*, 1996; Dowsett and Chu, 1998; Hofman, 1999; Dupuy, 1994). At this stage, the definition of  $\Delta z$  is somehow arbitrary and purely phenomenological. It mainly serves for comparison of depth resolution data obtained in different works and by different authors. Only, in the case of a Gaussian function the mathematical meaning is well defined by  $\Delta z$  (16 - 84%)  $\approx 2\sigma$ , or more exactly  $\Delta z$  (15, 87-84, 13%)  $\approx 2\sigma$ , where  $\sigma$  is the standard deviation of the Gaussian; the shape of the depth profile of the sharp A/B interface is an error function. One notes that the derivative of the normalized sharp interface profile is the resolution function. Other phenomenological descriptions consider that the depth resolution can be estimated by means of the Full Width at Half Maximum (FWHM) of a peak-shaped profile, which corresponds to  $2.355\sigma$ . (Herzel *et al.*, 1995; Gautier *et al.*, 1998, 1997).

These notions are not sufficient enough, because the Collisional mixing is not only responsible for a broadening of the real profiles, but also for the asymmetry which is represented mostly by an exponential-like tail (Hofmann, 2001; Gautier *et al.*, 1996; Dowsett *et al.*, 1994).

### FROM THE IN-DEPTH RESOLUTION TO THE DEPTH RESOLUTION FUNCTION, DRF

**Depth resolution function:** In principle, SIMS response function (or depth resolution function) can be obtained by profiling a single ideal impurity,  $\delta$ -layer, grown in a substrate material. However, such a  $\delta$ -layer is an abstraction and even if it were not, there could be no means to recognize it. A measured response function will have a shape that is determined by a mixture of sample dependent and SIMS related effects. Thin layers of an adequate quality for response function measurement at probe energies above about 2 keV can be obtained (Dupuy *et al.*, 1994; Gautier *et al.*, 1998). But sample related structure becomes progressively a more significant part of a profile as the energy is reduced. This structure can result from steps in the  $\delta$ -layer across the analyzed area, the statistical distribution of atoms about the ideal depth, surface segregation during growth and finite diffusion; the contribution of these phenomena provides the Gaussian and exponential shape into the measured DRF.

The resolution function is a specific function that has to be determined for each set of experimental conditions. In the case of a SIMS experiment, the DRF changes each time the primary beam energy, the impact angle, the matrix or the impurity under investigation changes. In the case of the SIMS analysis of boron doped layers of silicon under  $O_2^+$  primary beam and with an oblique incidence angle (below  $30^\circ$ ), the collisional mixing is the responsible for a degradation of the depth resolution, that can be expressed in terms of a convolution of the original profile with a depth resolution function, DRF. This DRF, represented by the function  $h(z)$ , is the normalized response of a delta-doped layer when the analysis process is linear and invariant, that is when the resolution function does not vary with depth, which is true for depths ranging from  $\sim 150$  and  $8000 \text{ \AA}$  (Gautier *et al.*, 1996, 1998, 1997). A real concentration distribution  $x(z)$  will result in a measured profile  $y(z)$  defined by:

$$y(z) = \int_{-\infty}^{+\infty} x(z')h(z-z')dz' + v(z) \quad (1)$$

Where  $v(z)$  is the noise which adds independently to the perfect measured profile. The linearity of the process is

verified so long as the concentration, of the boron-doped layer, stays below the dilute limit (Gautier *et al.*, 1996). Thus, the assumption on which SIMS analysis can be described in terms of the convolution of an initial profile with a DRF that depends on the instrument and the analysis conditions seems to be valid, as has already been pointed out by Dupuy *et al.* (1994).

It is easy to see that if the input signal is a delta function, then  $y(z) = h(z)$ . The DRF can thus be found from the measurement of a delta function. This function has to be determined for each specific combination of matrix, impurity and experimental conditions. From a practical point of a view, the elaboration of a delta-doped structures of uniformly doped layers with ultra sharp interfaces is better controlled (Dupuy *et al.*, 1994) so that it is possible to get the DRF from the measurement of a Rapid Thermal Chemical Vapor Deposition (RTCVD) grown sample, which can be supposed to be very abrupt and very thin. The convolution/deconvolution process can be performed with a numerical DRF, experimentally determined. Another way is to use an analytical function that perfectly fits the experimental data; this method leads to some advantages (Gautier *et al.*, 1997; Dowsett and Collins, 1996).

- The sampling interval of the analytical DRF can be easily adjusted to match that of other experimental profiles to be deconvolved, especially where the erosion rate is not exactly the same as in the initial DRF measurement.
- If the DRF is experimentally measured for a lot of energies, it is possible to determine the variation of the fitting parameters, with respect to the energy: A better determination of these parameters for a given energy can be obtained by checking a continuity criterion.
- The possibility of describing the depth resolution with an analytical expression, via its moments, makes the performance of the analysis more comparable for different users working with different apparatus.
- The noise in the DRF is smoothed out (we can assume that the noise is a consequence of the measurement and not an inherent parameter of the DRF). Thus some of the artifacts in the result of the deconvolution can be avoided.
- One is free to choose the extent of the analytical DRF so that the fitting covers only the experimental data (in that case, the dynamic range of the analytical DRF is the same as the experimental one) or to extrapolate the DRF to simulate a very large dynamic range.

In the first case, the use of an analytical function is just a smoothing of the analytical data. It is as well the

case where there is no reason why the analytical form should not be implemented in a convolution or in deconvolution scheme, as claimed by Dowsett and Collins (1996). In this sense, it is assumed that the sample is a real data layer (MBE-grown sample are known to be very abrupt) and that the entire response is due to the measurement process.

When looking at a SIMS profile of a delta-doped layer of boron in silicon, we notice that it comprises an exponential trailing edge and a Gaussian-like rounded top. The rising part of a profile is often exponential too, although it is why we have chosen to implement an analytical DRF, initially proposed by Dowsett *et al.* (1994) which is constituted by the convolution of a double exponential with a Gaussian.

$$Dexp(z) = A \cdot \begin{cases} \exp(-\frac{z-z_0}{\lambda_u}) & z < z_0 \\ \exp(-\frac{z-z_0}{\lambda_d}) & z > z_0 \end{cases} \quad (2)$$

and

$$Gauss(z) = \frac{B}{\sqrt{2\pi}\sigma_g} \exp(-\frac{z^2}{2\sigma_g^2})$$

The result of this convolution is given by the normalized expression (Dowsett *et al.*, 1994; Dowsett and Chu, 1998):

$$h(z) = \frac{1}{2(\lambda_u + \lambda_d)} \left\{ \begin{array}{l} \exp(-\frac{z-z_0}{\lambda_u} + \frac{\sigma_g^2}{2\lambda_u^2}) \operatorname{erfc}(\frac{z-z_0}{\sqrt{2}\sigma_g} + \frac{\sigma_g}{\sqrt{2}\lambda_u}) + \\ \exp(-\frac{z-z_0}{\lambda_d} + \frac{\sigma_g^2}{2\lambda_d^2}) \operatorname{erfc}(-\frac{z-z_0}{\sqrt{2}\sigma_g} + \frac{\sigma_g}{\sqrt{2}\lambda_d}) \end{array} \right\} \quad (3)$$

This DRF can be described by three parameters  $\lambda_u, \lambda_d, \sigma_g$  and a fourth parameter  $z_0$  that represents the position of the cusp of the double exponential.

**Experimental determination of the resolution function:**

Figure 1 gives an example of this DRF experimentally measured and its fitting by the analytical expression in the range of the available energies and angles. The experiments have been carried-out with CAMECA Ims6f apparatus with  $O_2^+$  primary ions, collecting the positive secondary ions. This DRF has been measured in the case with of a delta layer of Si:B in silicon at 5.5 Kev/ $O_2$  and 9.5 Kev /  $O_2^+$  in Cameca IMS6f with positive secondary ion collection. The fitting parameters are not expressed with respect to the primary ion energy but with respect to

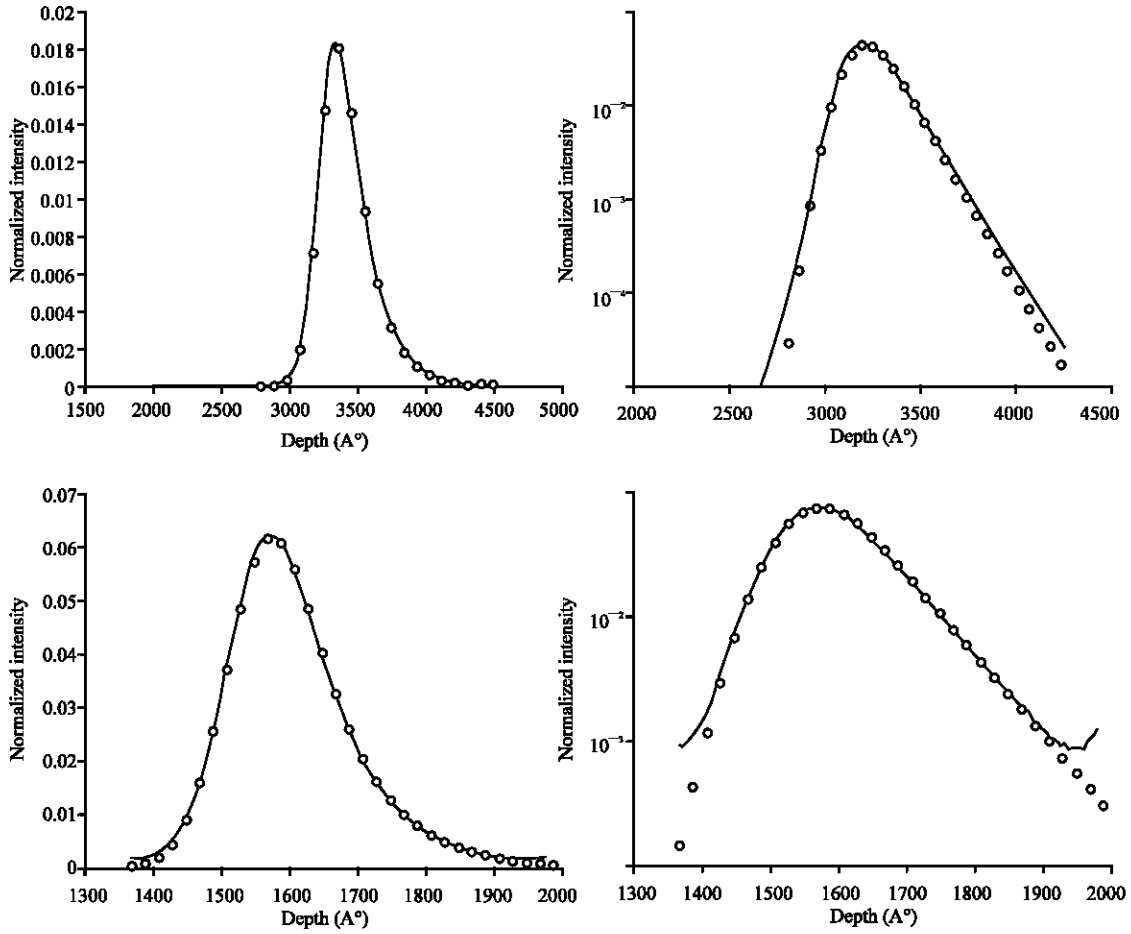


Fig. 1: Fitting of the resolution function by the analytical expression (normalized function) full lines: Experimental curve; circle: Fitting. 5.5 keV/O<sub>2</sub><sup>+</sup> primary beam, a) linear scale, b) logarithmic scale; 9.5 keV/O<sub>2</sub><sup>+</sup> primary beam, c) linear scale, d) logarithmic scale

the primary ion range,  $R_p$ , given by the formula (derived from TRIM simulation using O<sup>+</sup> ions with the same impact angles (Dupuy *et al.*, 1998):

$$R_p(A^\circ) = 50.46 E_p^{0.665} \cos \theta \quad (4)$$

Where  $\theta$  is the implicit angle of the beam and  $E_p$  is the primary energy per incident oxygen ion. This representation has been chosen in order to have synthetic results taking into account both energy and the angle of impact, which are not independent in a magnetic sector instrument. The variation of  $R_p$ , with respect to the primary ion energy  $E_p$ , is illustrated on Fig. 2. The variation of the fitting parameters when changing the experimental conditions conforms to the behavior of their physical homologue. We notice in particular the increase of  $\lambda_d$  and  $\sigma_g$  with  $R_p$ , however  $\lambda_u$  seems to decrease slightly with  $R_p$  (Fig. 3) (Gautier *et al.*, 1998). Thanks to the analytical form of the resolution function, we can

determine the mean value of  $h(z)$  by the first-order moment,  $\mu_1$ , the second-order moment  $\mu_2$  represents the in-depth resolution (Dupuy *et al.*, 1994; Gautier *et al.*, 1998).

$$\begin{aligned} \mu_1 &= \bar{z} = \lambda_d - \lambda_u \\ \mu_2 &= \sigma_{tot}^2 = \sigma_g^2 + \lambda_d^2 + \lambda_u^2 \end{aligned} \quad (5)$$

Knowing that the  $n$  order of the centered moment of a function is defined as:

$$\mu_n = \int_{-\infty}^{+\infty} (z - \bar{z})^n h(z) dz \quad (6)$$

By extrapolating the fitting parameters  $\lambda_d$ ,  $\lambda_u$  and  $\sigma_g$ , is possible to extrapolate the shape of the resolution function.

Equation 7 can then be rewritten as:

$$y = Hx + v \tag{8}$$

Where vectors  $y$ ,  $x$  and  $v$  represent, respectively: The observed profile, the true profile and the noise. The operator  $H$  is a Toeplitz matrix constructed from the discretized resolution function.

**The circular convolution:** The circular convolution product defined for the convolution of 2 periodic functions of  $N$  sample's period is noted:

$$y(z\Delta) = \left[ \sum_{k=0}^{N-1} h(k\Delta)x(z-k)\Delta \right] + v(z\Delta) \tag{9}$$

Computers can only manipulate vectors of limited sizes. Therefore, it is necessary to use functions of finished lengths; this is the case of the circular convolution product. In the linear convolution, the length of  $y$  is  $N_y = 2N-1$ , on the other hand the Eq. 9 indicates that  $y$  is of  $N$  length. Therefore, to get by the circular convolution a precisely result similar to the one reached by the linear convolution, it is sufficient to suppose that all vectors have a length equal to  $N_y$ , i.e., we must complete  $x$  and  $H$  by zeros, so that they reach this length. The obvious advantage of the circular convolution product is to limit the length of the convolution calculations to a finished value of points, without altering the result.

Fig. 2: Evolution of the primary ion range,  $R_p$ , with the primary ion energy  $E_p$

Fig. 3: Evolution of the fitting parameters, of DRF, with the primary ion range  $R_p$

**THE CONVOLUTION PROCEDURE**

**The linear convolution:** The discretization of the convolution integral (Eq. 1) results in the following equation, written with the matrixial formalism:

$$y(z\Delta) = \left[ \sum_{k=0}^{N_h-1} h(k\Delta)x(z-k)\Delta \right] + v(z\Delta) \tag{7}$$

$$N_y = N_x + N_h - 1$$

Where  $N_x$ ,  $N_h$ ,  $N_y$  and  $\Delta$  are, respectively the length of: the true profile, the resolution function array, the measured profile and the depth step. The depth step represents the rate erosion which is considered constant.

In this equation, the DRF is assumed to be causal, i.e., it corresponds to a delta layer located at  $z = 0$ , this does not corresponds to the physical situation and will shift the result of the profile.

**THE SIMULATION PROCEDURE**

The simulation procedure can be described as follows: Analytical functions of different structures are convolved with the analytical expression of the DRF with parameters  $\lambda_b$ ,  $\lambda_u$  and  $\sigma_g$ , having been determined previously by fitting the measured profile of a  $\delta$ -layer of boron in silicon. The simulated profiles are constructed so that they resemble to a real SIMS analysis of:  $\delta$ -layer, multi- $\delta$ -layer, Gaussian functions, rising and failing sharp functions, etc... and expressed in terms of ion counts per second. The maximum ion count of profiles is located in the range  $10^4$ ,  $10^5$  counts per second. Some Gaussian noise is subsequently added in order to simulate the real SIMS analysis. To simulate the noise that comes to be added to the perfect signal, we are have constructed a Gaussian noise with a mean value equal to zero and a standard deviation following the practical relation already used by authors (Gautier *et al.*, 1998).

$$\sigma = 1.7\sqrt{M} \tag{10}$$

Where M is the mean value of this signal.

It is necessary to think, first of all, about the generation of pseudo-random signal of a Gaussian distribution. In fact, the pseudo-random signals are perfectly deterministic signals, but whose behavior appears uncertain; these signals possess an interesting and very definite statistical properties. Such signals are generally generated to simulate the random signals and have a periodic character but on one period, it can be treated like a purely uncertain signal. For this reason, the period must be chosen as long as possible. In fact, the kind of noise in SIMS analysis is White Poissonian, this noise is weak in the case of pure coating. Moreover, it has been chosen that the noise is White Gaussian with a mean value equal to zero (i.e., the variation due to the noise, compared to what could be called a perfect measured signals and it can be either positive or negative, with a symmetrical probability distribution function). Brice have verified that the construction of a Poissonian noise that they added to the signal instead of a Gaussian noise does not lead to any difference in the deconvolution results. So it is preferable to use a Gaussian noise for several reasons:

- The Gaussian noise is far easier and faster to compute than the Poissonian noise.
- A Poissonian stochastic variable of the parameter  $\alpha$  will be able to be estimated by a Gaussian law for SIMS signals of the order of  $10^2$  to  $10^5$  counts per second, i.e.  $\alpha \gg 1$  (Gautier *et al.*, 1997; Makarov, 1999).
- In the regions where the SIMS signal is meaningful, it is very unlikely that the measured noise at the end of the profile represents a major contribution of the total noise.

Whenever, the number of counts becomes too low (<1cps) the mean value of the noise has been kept at unity so that the signal is covered by the noise, just as in a real SIMS experiment. This corresponds to rather pessimistic experimental conditions, for the mean level of the noise at the end of an experimental profile is often <1 cps. The noisy profile show a Signal-to-Noise Ratio (SNR) of 40 dB, which corresponds to credible SIMS analysis where four decades of signal are available. Here, the SNR (dB) is expressed in terms of the ratio between the power of the signal and the power of the noise, which means that:

$$SNR = 10 \log_{10} \frac{\|y\|^2}{\|v\|^2} \tag{11}$$

This results in profiles that are rather similar to what can be obtained in a real SIMS experiment.

**The deconvolution procedure:** Different methods of deconvolution exist which offer advantages and drawbacks. There are: inverse methods based on Fourier transformation and forward methods. Inverse techniques are very fast but suffer from some essential drawbacks: They often give a result containing physically unrealistic negative concentration and high noise levels. Therefore, the solution is not unique and not stable (a little perturbation in the data can lead to a great difference in the deconvolved solution). The deconvolution procedure tries to find a unique solution and to stabilize it with respect to a perturbation in the data.

The algorithm that we have chosen, for the deconvolution of SIMS depth profiles, is Wiener algorithm. This algorithm is member of the set of those using inverse Fourier transforms, it is a flexible algorithm permitting the deconvolution of profiles with good gains in resolution and in amplitude.

Equation 8 can be re-written in Fourier space as:

$$Y_n(f) = Y(f) + N(f) \tag{12}$$

Where  $Y(f) = H(f)X(f)$  represents the ideal case, which no noise is present in the measurement (which is never the case).

The system response  $H(f)$  is a low-pass filter (Gautier *et al.*, 1998; Dowsett and Chu, 1998; Hofman, 1999; Cooke *et al.*, 1996; Makarov, 1993; Prost and Goutte, 1984). Its components are thus equal or very close to zero for frequencies above a certain cut-off frequency  $f_c$  (Fig. 4). Components close to  $f_c$  are very attenuated by the convolution. Moreover, in the presence of an ill-posed problem, some components below  $f_c$  can be very small, almost null. In this case, the inversion of the convolution equation will fail for these components. Therefore, it will have the same effect that the application of a high-pass filter, what will provoke the amplification of the high frequencies of the noise which will lead to a very unstable solution, therefore, the result is a signal drowned in the noise (Fig. 5). In these conditions, a solution is the application of a filter on the deconvolved signal, in which this amplification of the high frequencies will be minimized. One of the simplest manners of this type of restoration is to use the filter of Wiener; it is an extremely fast deconvolution because it is applied in the Fourier space and requires only a TF and an inverse TF. Therefore, the problem will be to find the optimal filter that, when it is applied to the result of the deconvolution, will give the result close to the searched input signal  $X(f)$ .

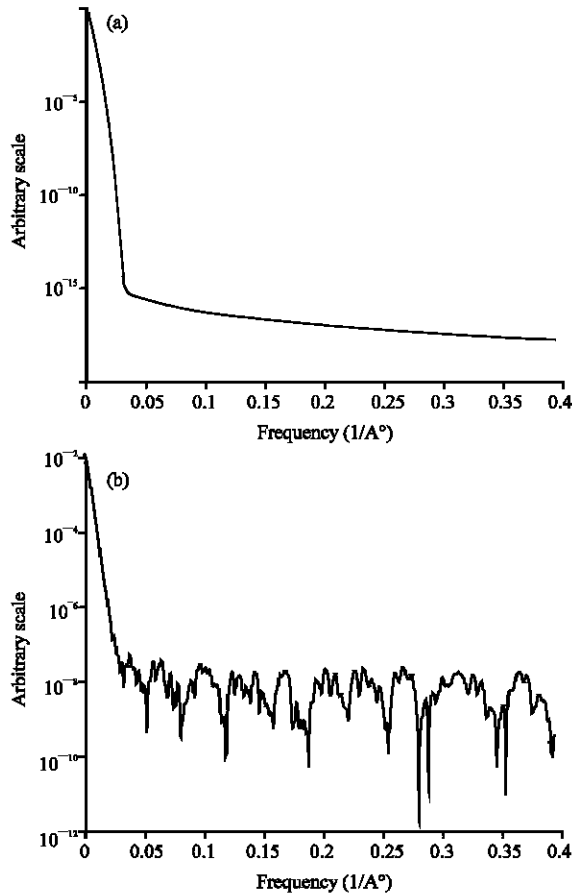


Fig. 4: Direct Fourier Transform (DFT) of the resolution function (a) analytical DRF, (b) experimental DRF

Fig. 5: Brute Deconvolution of a Gaussian profile by simple inversion of the convolution equation. The result is a profile drowned in the noise

In other words, one looks for the filter  $F(f)$  as:

$$X_{est}(f) = \frac{Y_n(f)}{H(f)} F(f) \quad (13)$$

Where  $X_{est}(f)$  represents the estimated of the real signal. It remains to define what one says by close to. The most natural definition is the approximation of the estimated solution  $X_{est}(f)$  by least squares with the true solution  $X(f)$  which will lead to minimize the quantity (Schafer *et al.*, 1981; Barakat *et al.*, 1997).

$$\int_{-\infty}^{+\infty} |X_{est}(f) - X(f)|^2 df \quad (14)$$

We note that the measured signal  $Y(f)$  and the noise  $B(f)$  are completely no-correlated. Therefore, the integral of their correlation product on  $f$  is null. To minimize the Eq. 14 while making vary  $F(f)$  it is sufficient to derivate it with respect to  $F(f)$  and to equal the gotten quantity to zero, that, finally, gives the estimated solution of Wiener:

$$X_{est}(f) = \frac{Y_n(f)}{H(f)} \frac{1}{1 + \frac{|N(f)|^2}{|Y(f)|^2}} \quad (15)$$

According to the Equ 11, the research of the best SNR (for real profile where it's value is unknown) has been done, in an empiric manner. One tries different values of the SNR and one takes the one that gives the best result.

## RESULTS AND DISCUSSION

**Rising and failing sharp functions:** The first kind of rising and failing functions, we have chosen to simulate, are sharp interfaces. This case is presented in the technology MOS, (Metal-Oxide-Semiconductors) with a great control of layer's deposition (for example LP-CVD or RT-CVD grown layers) to have abrupt interfaces.

The mathematic formulations of these structures are: For the increase sharp function we have:

$$C(z) = AU(z-a) = \begin{cases} A & z > a \\ 0 & z < a \end{cases} \quad (16)$$

For the decrease sharp function we have:

$$C(z) = A[U(z) - U(z - a)] \quad (17)$$

Where  $A$  is the amplitude coefficient represents the level of the signal and  $a$ : Is a shift introduced to the function, it represents the depth of the beginning of the sharp interface. We have chosen to make this study with a DRF corresponding to 5.5 keV/O<sub>2</sub><sup>+</sup> primary beam (42.4°

incidence) because it represents a routine adjustment of the instrument. Thus, we have convolved our theoretical profiles with a DRF that has an FWHM equal to  $97.83\text{A}^\circ$  ( $\lambda_d = 35.1\text{A}^\circ$ ,  $\lambda_n = 11.4\text{A}^\circ$ ,  $\sigma_g = 19.8\text{A}^\circ$  and  $\sigma_T = 41.88\text{A}^\circ$ , where  $\sigma_T$  is the centered second order moment of DRF). In the low frequencies of each profile we have added the noise with an SNR = 35 dB, for the failing sharp function, the noise affect the pure signal at the end, however for the other signal, the noise is localized at the beginning of the signal.

Figure 6 (a-d) show both sharp interfaces functions for  $A = 10^4$  cps and  $a = 800\text{A}^\circ$  and the result of the simulation of the SIMS analysis corresponding to a  $5.5\text{keV/O}_2^+$  primary beam in a linear and a logarithmic scale. It turns out that the abrupt interfaces became graduals, spread in depth following an error function. Following, it is the effect of the collisional mixing in return for the parameter  $\lambda_d$ . The usual  $\Delta z$  (16-84%) definition can, of

course, be applied to any profile at a sharp interface of a single-layer structure when the maximum and the minimum of plateau values are attained. However, it's simple and well-defined meaning for a Gaussian DRF ( $\Delta z = 2\sigma$ ) is lost in the case of a non-Gaussian resolution function. For example, the exponential decay generally obtained due to collisional mixing within a mixing length  $w$  shows that  $\Delta z(16-84\%) = 1.6w$  (Hofman, 1999). With our DRF;  $\Delta z(16-84\%) = 77.88\text{A}^\circ$  for the failing sharp interface and it equal to  $76.03\text{A}^\circ$  for the rising sharp interface. Indeed, we nearly have the same resolution in depth, with a difference of  $1.85\text{A}^\circ$ . Consequently, the width of the mixed zone is, in the two cases, equal roughly to  $w \approx 47\text{A}^\circ$ .

The degradation resulting from the measure of a sharp function, either rising or failing, carries essentially on the increase and the decrease part of the signal, which appear as exponential tails on the measured profile. The deconvolution leads to a significant improvement of the SIMS analysis (Fig. 6 a-d). In particular the sharpness of

Fig. 6: Results of the deconvolution of SIMS sharp interfaces profiles: -Rising sharp interface: (a) Linear scale, (b) logarithmic scale. -Failing sharp interface: (c) Linear scale (d) Logarithmic scale. Some oscillations appear on both scales. The exponential behavior of the measured profile has been removed



different interfaces is retrieved and the quality of the signal is mostly improved. In this type of sample, the means to estimate the quality of the deconvolution is to compare the different in-depth resolutions, characterized by the  $\Delta z$  (16-84%) criterion, of the deconvolved profiles with those of the measured profiles. The deconvolution gives the following in-depth resolution for each profile  $\Delta z$  (16-84%) = 16.58Å and  $\Delta z$  (16-84%) = 18.43Å, respectively, which gives an improvement by a factor over of 4.2 for each case. However, on the plateau of each profile, i.e., in the high level of the signal, some oscillations appear and at the end of each profile, artifacts are developed at the low level of the signal. The question for the SIMS analyst is to know whether these disruptions (artifacts, oscillations) are to be considered as physical features or as deconvolution features (Gautier *et al.*, 1996). We will try to find an explanation of these phenomena later.

**Error functions:** The second kind of rising and failing functions we have chosen to simulate are error functions, often encountered when a diffusion process is involved. A Fickian diffusion of an abrupt interface results in an error function-like profile. The general formulation of the functions that we have constructed is:

$$C(z) = \frac{C_0}{2} \left[ 1 \pm \operatorname{erf} \left( \frac{z}{\sqrt{2}\sigma_0} \right) \right] \quad (18)$$

Where  $C_0$  is the amplitude coefficient used to adjust the level of the signal and  $\sigma_0$  characterizes the abruptness of the profile. The total profile is constituted by a rising and a failing error function. Figure 7 Shows the function for  $\sigma_0 = 28.5\text{Å}$  and the result of its convolution with a DRF corresponding to a 5.5 keV/O<sub>2</sub><sup>+</sup> primary beam in a linear and a logarithmic scale.

We notice also that, the primary ion range of the analysis characterized by  $2R_p$  (Gautier *et al.*, 1996) in our case  $R_p = 74 \text{Å}$ , the transient response influences on the first rising part, but not in an ominous manner, on the other hand in the second part of the signal, the primary ion range is drowned in the noise, this it is an advantage for this kind of profiles (i.e., rising functions). Also, in this figure, it can be seen that the SIMS analysis broadens the rising and the failing function of each signal and particularly that the failing error function because the measured signal is governed mostly by the decreasing exponential behavior of the DRF.

The result of the deconvolution of this signal can be found in the same Fig. 7. In our case where  $\sigma_0 = 28.5 \text{Å}$ , the signal is almost perfectly deconvolved in its rising and

Fig 7: Results of the deconvolution of error functions profiles: (a) Linear scale, (b) Logarithmic scale. Dotted line: original profile. Plain line: Deconvolved profile. Noisy line: Measured profile. The deconvolution is perfect: On the linear scale, the original signal can not distinguished from the deconvolved signal. Some oscillations are visible on the logarithmic scale

failing parts. In the region where the signal is constant, some oscillations are visible in a linear scale, they are characteristic of the result when the process of deconvolution reaches its limits, that means; when the profile to recover contains too high frequencies to be restored by the algorithm. On the other hand, in logarithmic scale (Fig. 7 b) artifacts are developed in the low levels of the signal, where the signal is comparable to the noise are normal and unavoidable. There are due to the local variations of the mean value of the noise. It turns out that the depth resolution is improved in a very satisfactory way, this is justified by a completely restoration of the measured profile which is close to the original profile.

Fig. 8: Results of the deconvolution of Gaussian profiles:-  $s_R = 10\text{\AA}^\circ$ : (a) Linear scale, (b) Logarithmic scale; -  $s_R = 120\text{\AA}^\circ$ : (c) Linear scale, (d) Logarithmic scale; The deconvolution is perfect in the second profile ( $s_R = 120\text{\AA}^\circ$ ) the original profile can not distinguished from the deconvolved signal, a small peak is visible on the right side on logarithmic scale

**Gaussian profile:** The Gaussian profiles which often appear after a diffusion process, are modified by the SIMS analysis, are represented on Fig. 8 (a-d). It is easy to see that when the standard deviation  $\sigma_R$  of the original profile to be analyzed is weak compared to the standard deviation of the DRF, it is very difficult to estimate  $\sigma_R$  from the SIMS analysis. For higher values of  $\sigma_R$ , the result of the convolution is characterized by a broadening mostly governed by  $\sigma_R$ , with rising and falling tails governed by  $\lambda_u$  and  $\lambda_d$ . In any case, it is possible to precise the analytical shape of the measured profile (Gautier *et al.*, 1996, 1997).

The DRF is represented by  $h(z)$  which consists in the convolution of the double exponential function  $\text{Dexp}(z)$  with the Gaussian  $\text{Gauss}(z)$ . We have from Eq. 8, the analysis of a real concentration distribution

$$x(z) \text{ is } y(z) = h(z)*x(z)$$

Which we can develop as:

$$y(z) = [\text{Dexp}(z)*\text{Gauss}(z)]*x(z) \quad (19)$$

This expression can be written as:

$$y(z) = \text{Dexp}(z)*[\text{Gauss}(z)*x(z)] \quad (20)$$

Now, in the case where  $x(z)$  is a Gaussian,  $[\text{Gauss}(z)*x(z)]$  is also a Gaussian with a standard deviation.

$$s_T^2 = s_R^2 + s_G^2 \quad (21)$$

The result of the convolution of a Gaussian with the DRF has thus the same analytical shape as the DRF, that is the result of the convolution of a double exponential  $\text{Dexp}(z)$  with a Gaussian characterized by its standard deviation  $\sigma_T$ . An important property of the resolution function is the conservation of the centered second order moment in its quadratic form, even if the functions under

consideration are not Gaussian, it can thus always be written as:

$$s_M^2 = s_R^2 + s_{DRF}^2 \quad (22)$$

Where  $s_M^2$ ,  $s_R^2$  and  $s_{DRF}^2$  are, respectively, the centered second order moment of: The measured profile, the real profile and the DRF. In the general case, it is theoretically possible to find the centered second order moment  $\sigma_M$  when  $\sigma_R$  and  $\sigma_{DRF}$  are known.

Figure 9 (a) represents the measured centered second order moment as a function of  $\sigma_R$ . A good agreement is found between the  $\sigma_M$  measured directly with the convolved function and the  $\sigma_M$  deduced from Eq. 22. The inverse operation which consists in finding  $\sigma_R$  from  $\sigma_M$  is of course limited to the value of  $\sigma_R$  not too small compared to  $\sigma_{DRF}$ , for example, a measured  $\sigma_M$  of  $109 \text{ \AA}^\circ$  allows to find  $\sigma_R \approx 107 \text{ \AA}^\circ$ , however, the original  $\sigma_R = 100 \text{ \AA}^\circ$ , what gives us an error of  $7 \text{ \AA}^\circ$ . But a measured  $\sigma_M$  of  $46 \text{ \AA}^\circ$  allows to find  $\sigma_R \approx 40 \text{ \AA}^\circ$ , the original  $\sigma_R = 10 \text{ \AA}^\circ$ , what gives us an error of  $30 \text{ \AA}^\circ$ . It is important to note that when  $\sigma_R$  is not very different from  $\sigma_{DRF}$ , or even for higher values, the error made when one supposes that  $\sigma_R \approx \sigma_M$  is not negligible. One often measures the FWHM, which is in this case directly proportional to the standard deviation. This procedure is theoretically not valid in the SIMS analysis, mostly because of the exponential tail induced by the analysis. However, in highest decade of the signal, the DRF is still mostly governed by its Gaussian component, the exponential tail being predominant when the level of the signal is getting low. We have thus verified that the quadratic additive was partially respected. We have proceeded the way we had already done when dealing with the centered second order moment, by measuring the FWHM of the numerically convolved functions. It is interesting to note that the property:

$$\text{FWHM}_M^2 = \text{FWHM}_R^2 + \text{FWHM}_{DRF}^2 \quad (23)$$

It is respected also, as it can be seen in Fig. 9b.

Results of the deconvolution of the original Gaussian profiles with ( $\sigma_R = 10 \text{ \AA}^\circ$ ,  $(\text{FWHM})_R = 23.36 \text{ \AA}^\circ$ ) and ( $\sigma_R = 120 \text{ \AA}^\circ$ ,  $(\text{FWHM})_R = 280.32 \text{ \AA}^\circ$ ) illustrated on the Fig. 8a-d, respectively. It can be seen that the FWHM of the measured profiles are completely recovered after deconvolution.

We call gain of the deconvolution, the ratio of the FWHM of the measured profile on the FWHM of the deconvolved profile (Gautier *et al.*, 1997). It gives directly an idea of the improvement of the resolution after

Fig. 9: a) Evolution of the standard deviation of simulated SIMS Gaussian profile according to the standard deviation of the original profile. b) Evolution of the FWHM of simulated SIMS Gaussian profile according the initial FWHM of the original profile. Verification of the theoretical relations given by Eq. 25 and 26

deconvolution. The standard deviation and the FWHM of the measured profiles are, respectively ( $\sigma_M = 46.16 \text{ \AA}^\circ$ ,  $(\text{FWHM})_M = 107.84 \text{ \AA}^\circ$ ) and ( $\sigma_M = 128.18 \text{ \AA}^\circ$ ,  $(\text{FWHM})_M = 299.43 \text{ \AA}^\circ$ ). After deconvolution, features of each profile are respectively ( $\sigma_d = 10.36 \text{ \AA}^\circ$ ,  $(\text{FWHM})_d = 24.20 \text{ \AA}^\circ$ ) and ( $\sigma_d = 120.19 \text{ \AA}^\circ$ ,  $(\text{FWHM})_d = 280.64 \text{ \AA}^\circ$ ) which gives gains of deconvolution of 4.45 and 1.06, respectively. One notes also that, features of DRF are ( $\sigma_{DRF} = 41.88 \text{ \AA}^\circ$ ,  $(\text{FWHM})_{DRF} = 97.83 \text{ \AA}^\circ$ ). Therefore, we conclude that: it is possible to improve the in-depth resolution of the analysis by a factor greater than 4.4 when the original profile is less than DRF. It is still improved by a factor close to 1 when the measured profile is times larger than the DRF. To generalize this survey, we have deconvolved the same set of Gaussian profiles of various  $\sigma_R$  previously

between two deltas layers. The question of the in depth-resolution can also be posed in terms of the ultimate separability: If one considers two very fine layers, what distance do they have, to be separated, so that the measure can distinguish each of them? This approach of the resolution drives to more refined definitions, because it is necessary to specify the degree of separation of the two layers.

We use a separability criterion, indicated by the notation  $d_{(\%, \text{dB})}$  (Gautier *et al.*, 1996), as being the minimal distance required between two delta layers, so that the contrast obtained by the SIMS profile, blurred by the noise with an  $\text{SNR}_{(\text{dB})} = x \text{ dB}$  (Eq. 11) is given by:

$$C_{(\%)} = \frac{I_{\max} - I_{\min}}{I_{\max}} \times 100 \quad (24)$$

Where  $I_{\max}$  and  $I_{\min}$  are, respectively, the intensity at the maximum of the most intensive peak and the intensity in the valley separating the layers. It is interesting to find the minimum distance between two delta layers, convolved by the SIMS DRF and that can be separated by the analysis. In order to have a general point of view of the separation power of our analysis, we have constructed a theoretical samples consisting of two delta-layer separated by an adjustable distance ranging from 50 to 300Å and convolved with the DRF, added a Gaussian noise in order to obtain a signal with an SNR equal to 35 dB.

We have convolved our theoretical profiles with a DRF that has an FWHM equal to 97.83Å ( $\lambda_d = 35.1\text{Å}$ ,  $\lambda_v = 11.4\text{Å}$ ,  $\sigma_g = 19.8\text{Å}$  and  $\sigma_T = 41.88\text{Å}$ , where  $\sigma_T$  is the centered second order moment of DRF). The variation of the contrast according to the distance is illustrated on the Fig. 11a. It turns out that 2 delta layers are separated if they are separated by  $>115\text{Å}$ . We consider that the separation of the delta layers is perfect when the convolved curves do not intercept within the dynamic range investigated by the convolution. In the case where the SNR is equal to 35 dB, this range extend over four decades. After deconvolution (of course, with the same DRF which is used for the simulation) the real distance between peaks and the symmetry have been restored, indicating that the exponential behavior of profiles has been completely removed. Besides, the intensity peaks of the delta layers have been corrected so that both layers exhibit the same peaks (Fig. 12a-d).

The variation of the contrast, of the deconvolved profiles, with respect to the distance is illustrated on the Fig. 11b. The two delta-layers are perfectly separated if they are initially separated by a distance greater than 60Å, in these conditions and it is still possible to detect them if they are separated by more than 40Å, two delta-

Fig. 10: Plot of the variation of the: (a) Measured and deconvolved standards deviation with respect to the initial standard deviation.(b) Measured and deconvolved full width at half maximum with respect to the variation of the  $(\text{fwhm})_R$

simulated. For each deconvolved profile, we have noted the centered second order moment and the full width at half maximum. The result can be found in Fig. 10a and b. These Figures show that the real width of the Gaussian profile can be restored if the FWHM of the original profile is comparable or higher to the FWHM of the DRF. If it is narrower, the resolution can only be improved, but the result is far to the original profile. Brice *et al* got, practically, the same results with another algorithm of deconvolution, what validates this survey.

**Two layers separated with an adjustable distance:**

Generally, the response of a system is more large that the structure that one wishes to analyze. In some cases this width covers two consecutive structures, as two adjacent delta-layers. It has for result the observation of only one structure at the time of the measure. We have simulated the measure of two separated delta-layers of an adjustable distance to discover the theoretical separation limit

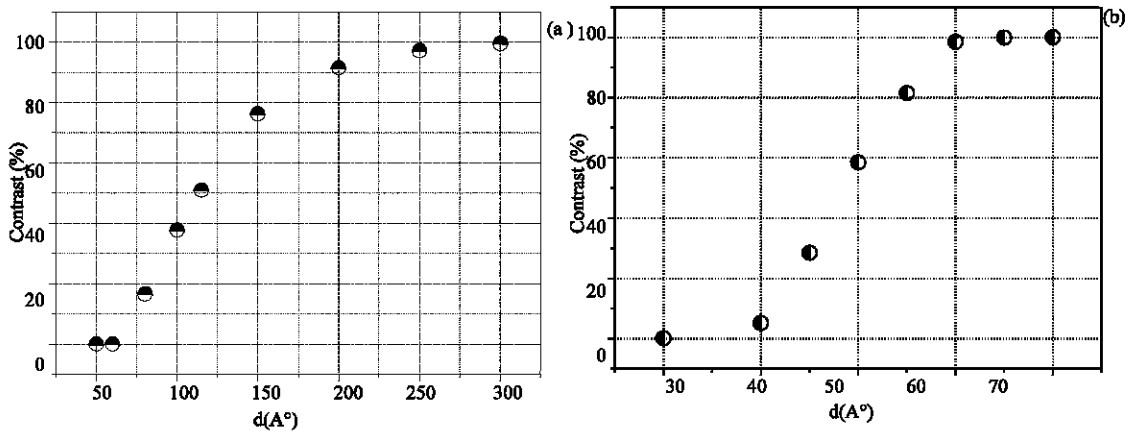


Fig. 11: (a) Evolution of the contrast with the distance separating two delta-layers. (b) Evolution of the contrast of the deconvolved profiles with the distance separating two delta-layers. Improvement of the in-depth resolution by deconvolution, limit of separation is equal to  $40 \text{ A}^\circ$

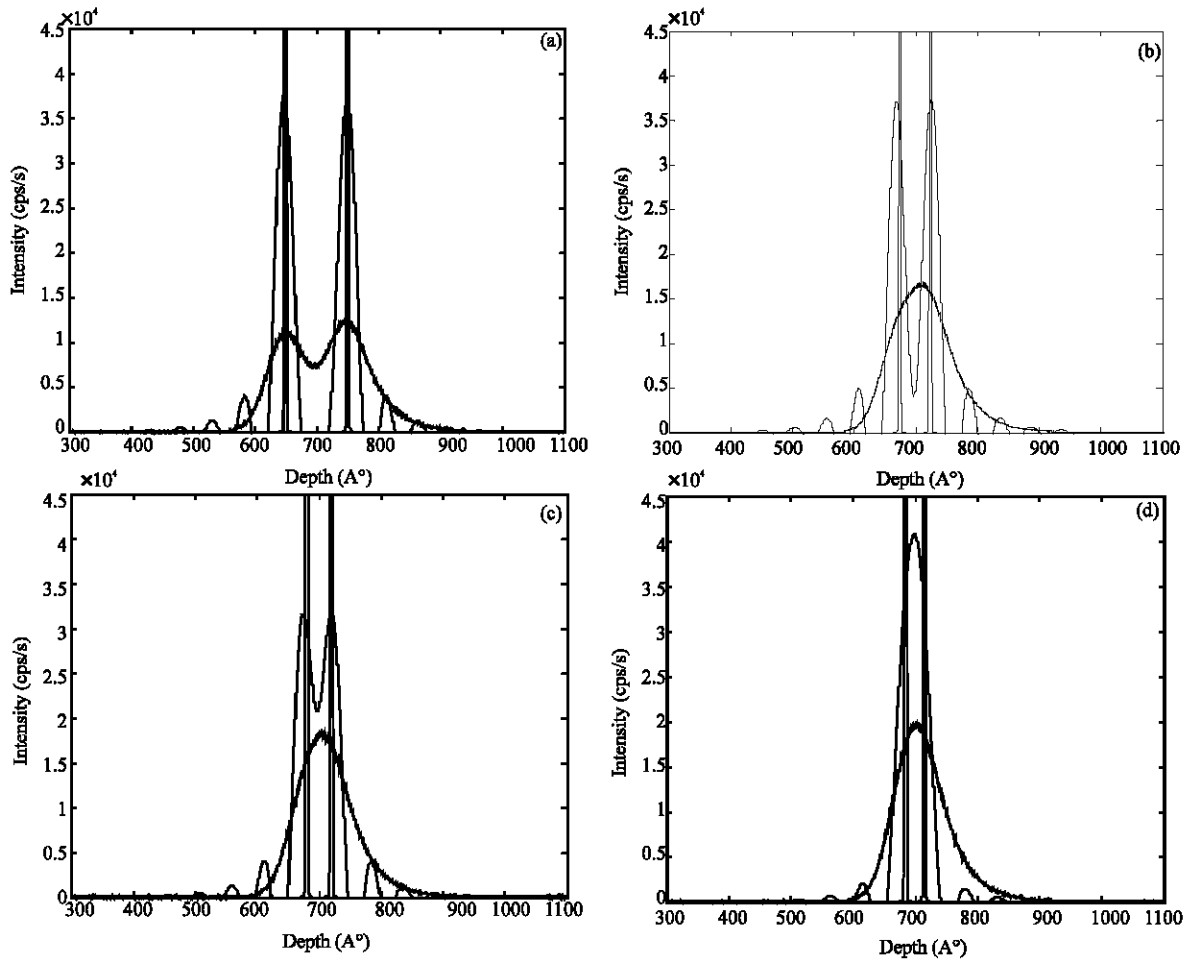


Fig. 12: Separation of two delta layers initially separated by: (a)  $60 \text{ A}^\circ$ , (b)  $50 \text{ A}^\circ$ , (c)  $40 \text{ A}^\circ$ , (d)  $35 \text{ A}^\circ$ . Dote line: Original profile, noisy line: Measured profile, plain line: Deconvolved profile

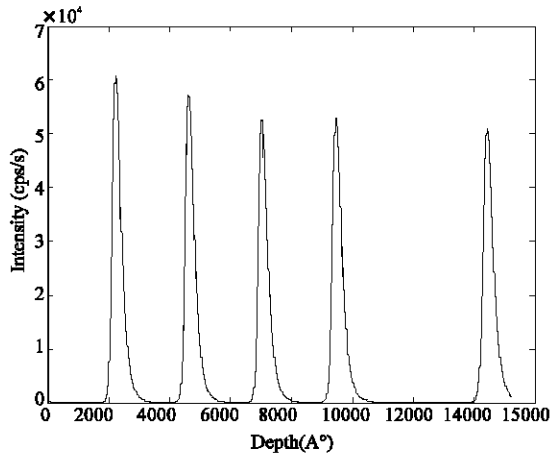


Fig. 13: Experimental SIMS depth profile of a sample consisting of five delta-layers of Si:B, 2.5 keV/O<sub>2</sub><sup>+</sup> (63.1° incidence)

layers separated by 35A° are not separable. In particular, these results can be considered as good, by comparison with Brice results (Gautier *et al.*, 1997) by means of the same separability criterion (Eq. 24) Brice *et al* present a resolution equal to 60A° and the two delta-layers are completely separated by a distance >90A°. However, results of Brice are more stable, there are no small peaks (artifacts) at both sides of the deconvolved peaks. Cook *et al.* (1996) present a resolution better than 50A° with a Quadripole instrument with 2Kev/O<sub>2</sub><sup>+</sup> primary beam at normal incidence.

**Real SIMS profiles: multilayer depth profiles:** In microelectronics, component's dimensions decrease of one day to the other with the passing of years, therefore interfaces in materials are more and more abrupt. Those results are of an increased presence of the high frequencies in the specter of the real profiles. The survey of the delta-layer is therefore of an essential interest for the convolution/deconvolution process. Besides, a delta-layer represents the smallest structure that one can simulate or measure. Multilayer structures are also of great importance of semiconductors devices and so have become popular as reference materials in sputter profiling, particularly for the determination of depth resolution as a function of the sputtered depth (Kawashima *et al.*, 2004; Hofman, 1999; Gautier *et al.*, 1995).

Figure 13 shows a real SIMS profile, it contains five delta-layers analyzed with Cameca Ims6f corresponding to 2.5 keV/O<sub>2</sub><sup>+</sup> primary beam (63.1° incidence). The convolution ratio (Gautier) will be defined as the ratio of the FWHM of the measured profile on the FWHM of DRF. It gives an idea of how difficult it will be to restore

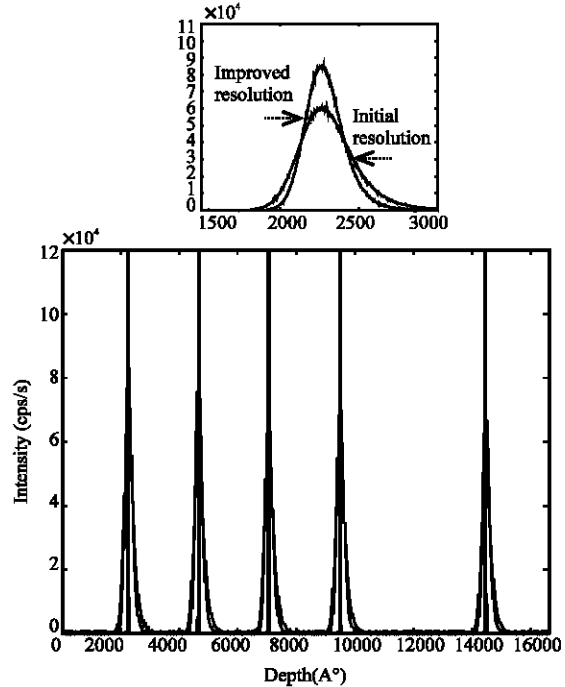


Fig. 14: Example of experimental improvement of in-depth resolution of multi-layer SIMS analysis by adjustment of DRF parameters (i.e. adjustment of operative's conditions). Parameters of the new DRF:  $\lambda_d=9.01$  A°,  $\lambda_n=1.9$ A°,  $s_g=8.9$  A° and  $s_T=12.84$ °

the measured profile after deconvolution. The closer to 1 the convolution ratio, is more difficult the restoration.

The FWHM of each delta-layer is equal to 43.8782A°, the one of the DRF is equal to 43.8169A°, relatively it is a good in depth-resolution, lower to 70A°, on the experimental plan that is a good measure, however, one stands in a difficult restoration because the ratio of the convolution is close to 1, precisely it equals to 1.0014. This value of the convolution ratio, allows us to test the validity and the performances of algorithms of the deconvolution, to have a better restoration of signals. Figure 14 shows the improvement of in-depth resolution. In these conditions, the operative conditions correspond to a fitting parameters of the DRF that has an FWHM equal to 30.0A° ( $\lambda_d=9.01$ A°,  $\lambda_n=1.9$  A°,  $\sigma_g=8.9$ A° and  $\sigma_T=12.84$ °). It turns out that the resolution is only improved by a factor equals to 1.34 and the dynamic range is improved by a factor 1.41. The improvement remains steady even while changing the operative conditions, i.e., lowering of the primary ion energies, in an other word, that explains the limits of the experimental improvement. Therefore, one has recourse to use other tools of improvement, which is the numeric improvement by deconvolution.

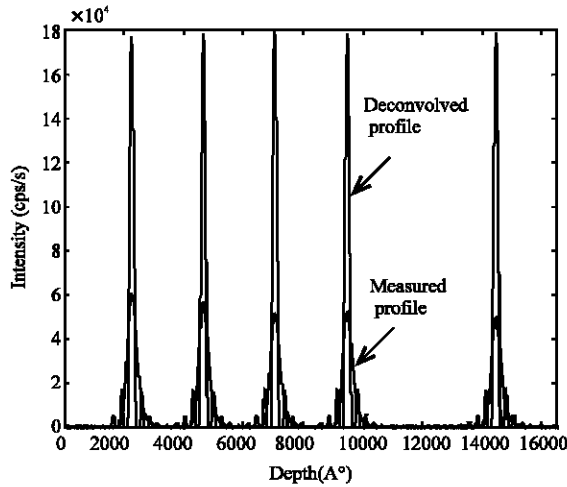


Fig. 15: Result of the deconvolution of the multilayer profile consisting of five delta layers. The deconvolution gives an excellent improvement of: The in-depth resolution, the dynamic range. All deconvolved peaks have the same height and are symmetric i.e. the exponential behavior of the measured profile has been removed

After deconvolution, Fig. 15, the delta layers are completely separated, although the SIMS analysis profile itself yields a poor separation, the shape of the result is symmetrical for all layers, indicating that the exponential features caused by the SIMS analysis are removed. The FWHM of the deconvolved delta-layers is  $14.74\text{A}^\circ$ , so the FWHM of the measured deltas is  $43.8782\text{A}^\circ$ , which gives a gain of deconvolution of 2.97, the dynamic range is improved by a factor of 4.14. These values are very satisfactory, in matter improvement of the quality of signal, which depend on several parameters: the used DRF in the deconvolution process, the method of the deconvolution, the step of sampling and the level of noise. Besides, the heights of the delta layers have been corrected so that all layers have approximately the same height, which the SIMS analysis modified them. As the previous cases, some artifacts are generated at the end of the deconvolved peaks, those have an amplitude of about one to 2 decades greater to the one of the noise. The interpretation is obvious, the useful signal to noise ratio in these zones is very bad, it is difficult to distinguish between the part of the signal and the part of the noise; one deducts a difficulty of deconvolving zones of a weak SNR. Also one notes that, these artifacts appear with other methods of deconvolution: regularized algorithm of Van Cittert, Maximum of entropy, etc. (Dowsett and Chu, 1998; Dowsett and Collins, 1996; Makarov, 1999; Schafer *et al.*, 1981; Barkat *et al.*, 1997; Mancina *et al.*, 1997).

## CONCLUSION

The aim of this survey is the improvement of the in-depth resolution of SIMS analysis. Several solution are to consider, the most classical known is the lowering of the primary ion energies which seems to be a good solution, but it is limited. That's why, the development of an alternative solution is needed to predict some SIMS measures, with better resolutions that the experience could not reach.

In this study, deconvolution of simulated and real profiles was considered. The simulation, based on the response function of the system, was undertaken. In this sense, the DRF was determined by analyzing delta-layer of boron doped silicon in silicon matrix and fitted by an analytical expression. The results of simulation are in good agreement with the experience. The real SIMS profile is a multilayer of boron in silicon analyzed at  $2.5\text{Kev}/\text{O}^+_2$  ( $63.1^\circ$  oblique incidence).

It is shown that the shape of all profile is retrieved in a very satisfactory way; the exponential behavior have been completely removed, the height of the delta-layers have been corrected, the distance between peaks and the symmetry have been restored. The in-depth resolution has improved by a mean factor supper than 3 in almost of profiles.

Ideally, what is obvious; it is that one can not replace a good measure by a numerical processing. Reliability and quality of the outgoing measure remained the essential requirement for a good result. All as the improvement of the instrumentation remains a privileged way toward the ultimate improvement of the in-depth resolution. The deconvolution comes to be added to the instrumentation performances and allows to pull the maximum of the resolution of an experimental profile.

This research shows that the deconvolution of SIMS depth profiles can be successfully used as a reliable way of improving SIMS in-depth resolution.

## REFERENCES

- Aitkaki, A., M. Boulakroune, M. Boukezata, M. Berrabah, F. Djahli, M.S. Bellatreche and D. Bielle-Daspet, 2002. *J. Semi. Cond. Sci. Tech.*, 17: 983-992.
- Boulakroune, B. and M. Berrabah 2001. *J. Sci. Tech.*, pp: 9-16.
- Barakat, V., B. Guilpart, R. Goutte and R. Prost, 1997. *J. Sign. l proc. IEEE.*, pp: 310-313.
- Cooke, G.A., M.G. Dowsett and P.N. Allen, 1996. *J. Vac. Sci. Tech.*, 14: 132-135.
- Cooke, G.A., M.G. Dowsett and P. Philipps, 1996. *J. Vac. Sci. Tech.*, 14: 283-291.

- Dowsett, M.G., G. Dowlands, P.N. Allen and R.D. Barlow, 1994. *J. Surf. Interface. Anal.*, 21: 310-322.
- Dowsett, M.G. and D.P. Chu, 1998. *J. Vac. Sci. Tech.*, 16: 377-381.
- Dupuy, J.C., G. Prudon, C. Dubois, P. Warren and D. Dutartne, 1994. *J. Nucl. Instr. Meth. Phys. Res.*, 85: 379-382.
- Dowsett, M.G. and R. Collins, 1996. *J. Phil. Trans. R. Soc. Lond.*, 354: 2713-2729.
- Gautier, B., R. Prost, G. Prudon and J.C. Dupuy, 1996. *J. Surf. Interface. Anal.*, 24: 733-745.
- Gautier, B., J.C. Dupuy, B. Semmache and G. Prudon, 1998. *J. Nucl. Instr. Meth. Phys. Res.*, 142: 61-376.
- Gautier, B., J.C. Dupuy, R. Prost and G. Prudon, 1997. *J. Surf. Interface. Anal.*, 25: 464-477.
- Gautier, B., G. Prudon and J.C. Dupuy, 1998. *J. Surf. Interface. Anal.*, 26: 974-983.
- Herzel, F., K.E. Ehwald, B. Heinmann, D. Kruger, R. Kurps, W. Ropke and H.P. Zeidel, 1995. *J. Surf. Interface Anal.*, 23: 764-770.
- Hofman, S., 1999. *J. Surf. Interface Anal.*, 27: 825-834.
- Hofman, S., 1993. *J. Appl. Surf. Sci.*, pp: 9-19, 70/71.
- Hofmann, H., 2001. *J. Thin solid films* pp: 336-342.
- Kawashima, Y., T. Ide, S. Aoyagi and M. Kudo, 2004. *J. Applied Surf. Sci.*, pp: 800-803.
- Makarov, V.V., 1999. *J. Surf. Interface. Anal.*, 27: 801-816.
- Mancina, G., R. Prost, G. Prudon, B. Gautier and J.C. Dupuy, 2000. In: *Proc. SIMS International Conference, SIMS. Brussels*, pp: 497-505.
- Makarov, V.V., 1993. *J. Surf. Interface. Anal.*, 20: 821-832.
- Remmerie, J. and H.E. Maes, 1985. *Spectromeca. Acta.*, 40: 787-793
- Prost, R. and R. Goutte, 1984. *J. Sign. proc. IEEE*, 7: 209-230.
- Schafer, R.W., R.M. Mersereau and M.A. Richards, 1981. *J. IEEE.*, 69: 432-464.
- Shao, L., J. Liu, C. Wang, K.B. Ma, J. Zhang, J. Chen, D. Tang, S. Patel and W.K. Chu, 2004. *J. Nucl. Instr. Meth. Phys. Res.*, pp: 303-306.
- Wu, A.T., 2006. *J. Physica C*. paper in Press.
- Yang, M.H., G.G. Goodman, 2006. *J. Thin solid films*, 508: 276-278.
- Zalm, P.C., 1995. In *Proc. SIMS International Conference, SIMS. Munster*, pp: 443-451.